SERVICE STRENGTH ASSESSMENT OF MACROSCOPIC IMPERFECTIONS IN CAST STEEL ALLOYS

M. Stoschka[1)], M. Horvath[2)], W. Mössler[2)], Florian Grün[1)]
[1)]Chair of Mechanical Engineering, Montanuniversität Leoben,
Franz Josef-Strasse 18, 8700 Leoben, Austria
[2)]Siemens Mobility Austria GmbH, Eggenberger Strasse 31, 8020 Graz, Austria

ABSTRACT

As macroscopic imperfections can be locally treated as notches, it is advisable to use established notch fatigue concepts to deduce the service strength of defect-afflicted cast steel alloys. Recently, an advanced local fatigue assessment method has been developed within the CD-Laboratory for 'Manufacturing Process based Component Design' at the Chair of Mechanical Engineering, Montanuniversität Leoben. This design procedure bases on the "Total Strain Energy Density" method (T-SED) and features a probabilistic assessment of planar defect projections. The method has been validated for large-scale, defect afflicted, specimens under constant amplitude loading. This contribution addresses the operational strength as variable amplitude loading for cast steel G12MnMo7-4+QT. In total, forty variable amplitude load tests were carried out covering block-load sequences as well as service-load signals from railway bogie measurements. It is demonstrated that the T-SED method is well applicable to calculate the service strength of cast steel samples under variable, uniaxial loading for varying bulk defect geometries. A damage sum of $D = 0.3$ is recommendable to meet the design limit curve of the investigated high-strength cast steel alloy.

KEYWORDS

Variable amplitude loading, high-strength cast steel, total strain energy density, bogie service load, resonance testing.

INTRODUCTION

Adjustable manufacturing process settings in cast components support the optimization of local microstructural properties as well as the degree of porosity for certain volumes. Hence, the manufacturing quality of the highly-stressed volumes can be tailored to meet the service load requirements, e.g. by locally increased cooling rates and reduced amount of porosity. In case of cast steel applications, such as bogie components, macroscopic imperfections are almost unavoidable due to the increased solidification window of the alloy. Up to now, no standardized fatigue assessment link to cast quality classes exists.
Therefore, it is obvious to use local fatigue approaches for macroscopic imperfections, as the arbitrarily shaped defect geometry can be evaluated locally as crack, or notch [1]. For threshold-based fatigue design, the 'Theory of Critical Distances' (TCD) is often utilized [2]. To assess fatigue in the medium life region, the evaluation distances have to be increased. An application of the TCD for macroscopic imperfections is given in [3]. Although the TCD is

directly applicable for each point of the projected defect convex hull, a drawback of the method is the necessary calculation of the local curvature and bisection vector. This vector sets the stress evaluation point in case of the point method, which has to be interpolated from the elastic stress field as available nodal results do not match with the local evaluation points. Aside, 'Notch Stress Intensity Factors' (N-SIF) can be used for fatigue assessment of each point of the projected defect shape, as illustrated in [4]. Finally, the 'Strain Energy Density' (SED) method features the notch fatigue strength based on the stress field in the vicinity of the notch tip [5]. All three local methods, TCD, N-SIF and SED can be equivalently used for fatigue assessment of bulk volume defects, as the computational basis is the same elastic stress field [6,7]. If the plastic SED contribution needs to be considered, one has to set-up a time-consuming non-linear simulation of the projected defect shape, or deduce the plastic fraction from Neuber's hyperbola. An extension of Neuber's rule for the multiaxial stress field at the notch tip is presented in [8], which features a rapid 'Total Strain Energy Density' (T-SED) fatigue assessment of macroscopic imperfections in cast steels.

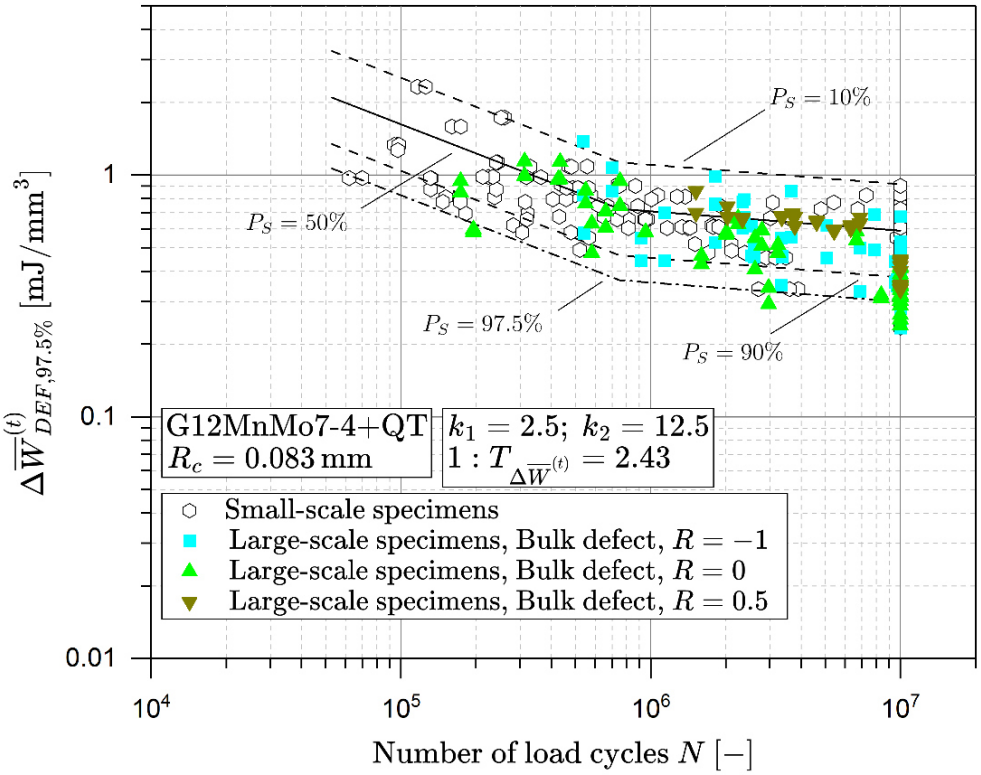

Fig. 1: T-SED small-scale specimen design limit curve of G12MnMo7-4+QT including CAL-results of large-scale specimens with bulk defects

The design limit curve of the investigated cast steel alloy G12MnMo7-4+QT is based on fatigue results of unnotched and notched small-scale samples, with opening angles of $2\alpha = 45°$ and $135°$, at stress ratios of $R = -1$, 0 and 0.5. In total, about one-hundred and eighty small-scale specimen results define the design limit curve in Fig. 1. In addition, constant amplitude loading (CAL) result of seventy-five large-scale samples containing bulk imperfections are sketched into the figure. For each imperfective large-scale specimen, two X-ray based planar imperfections are evaluated per sample. It is clearly recognizable in Fig. 1, that the CAL test results of large-scale specimens with macroscopic imperfections are within the proposed design limit curve.

The present paper extends the T-SED based investigations of cast steel G12MnMo7-4+QT towards service strength. Thus, several block-cycle based load cases are tested until burst fracture and evaluated against the given design limit curve. As a resonance test rig with block-cycle test programs is utilized, the course of the setpoint and actual force values are logged during testing. Based on the setpoint and measured force values, the change in computed T-SED is evaluated. In addition, closed-loop control settings of the resonance test rig are varied and especially the effect of the feedforward value at each new load block is studied in terms of overload peaks. Moreover, a given service load spectrum from bogie measurements is applied [9], which is realized by user-defined short load sequences for resonance test rig application and verified as transient set value in case of servo-hydraulic testing as well.

SPECIMEN, TEST RIGS AND LOAD CASE STUDIES

The geometry of the large-scale specimen is shown in Fig. 2. For each sample, the macroscopic imperfection geometry is obtained non-destructively as planar X-ray projections at two orthogonal levels.

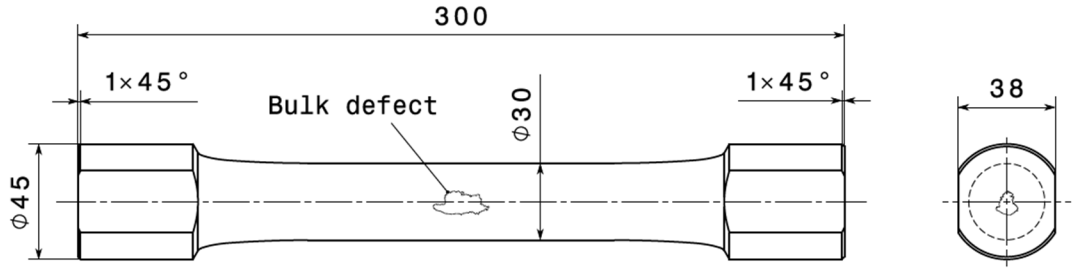

Fig. 2: Large-scale specimen geometry with bulk-defect [8]

Test rigs

The majority of the large-scale samples was tested uniaxially at a resonance test rig ‘Sincotec PowerSwing 600kN’. A few validation samples were tested at a servo-hydraulic test rig with a ‘MTS 244.51-1000kN’ cylinder. The test rigs are depicted in Fig. 3. The executed test frequency at the servo-hydraulic test rig is about $10Hz$, whereas the resonance test rig performs at 70 to $80Hz$, depending on the specimen stiffness and the requested load level.

Fig. 3: Resonance test rig, clamped sample, servo-hydraulic test rig

Block load sequence

To investigate the suitability of the developed T-SED method for variable loading, a block-load based test program is set-up. The applied resonance test rig supports only block program-based load sequences. The basic load sequence consists of seven blocks, covering stress ratios from $R = -2$ to 0.7. As the settling time of the force amplitude is bound to the controller settings of the test rig, a ramp-up time of about four seconds is needed. Thus, the chosen number of load cycles *N* per block is initially set as some thousands cycles in Table 1. This is denominated as a period fraction of one-hundred percent. To study the effect of reduced period length, implying that the settling time becomes more dominant, reduced period lengths of thirty and ten percent are included. This reduces the period cycle sum from 66000 down to 19800 and 6600, thereby increasing the effect of settling time. Finally, the effect of the feedforward control setting is studied for five and ten percent positive feedforward value as well.

Block number (1..7)	1	2	3	4	5	6	7
R [-]	0.5	-1	0	0.7	-1	-2	-1
ΔS [MPa]	100	250	150	75	250	300	250
N [-], period 100%	8000	16000	8000	6000	8000	12000	8000

Table 1: Load sequence definition for block loading with variable stress ratio

To study the service strength at constant stress ratio, a fully reversal Gaussian distribution is chosen. The stepping is set to a fixed number of load cycles to meet the requirements of settling time for resonant testing. The cumulative frequency sum is one-hundred thousand load cycles, the length of the shortest block three-hundred as given in Table 2. Only six blocks are defined as Gaussian distribution, but the sequence is mirrored to obtain a bathtub-like shape.

Block number (1..6)	1	2	3	4	5	6
ΔS [MPa]	161	321	417	498	564	650
N [-]	70000	20000	7000	2000	700	300

Table 2: Load sequence definition for Gaussian distributed block loading (to be mirrored)

Service load sequence

The investigated service load sequence is gathered from on-track measurements of railway bogies [9]. The deduced time-history consists of 2220 load cycles in the tumescent load range. Fig. 4 depicts the signal as well the rainflow results in terms of force set values.

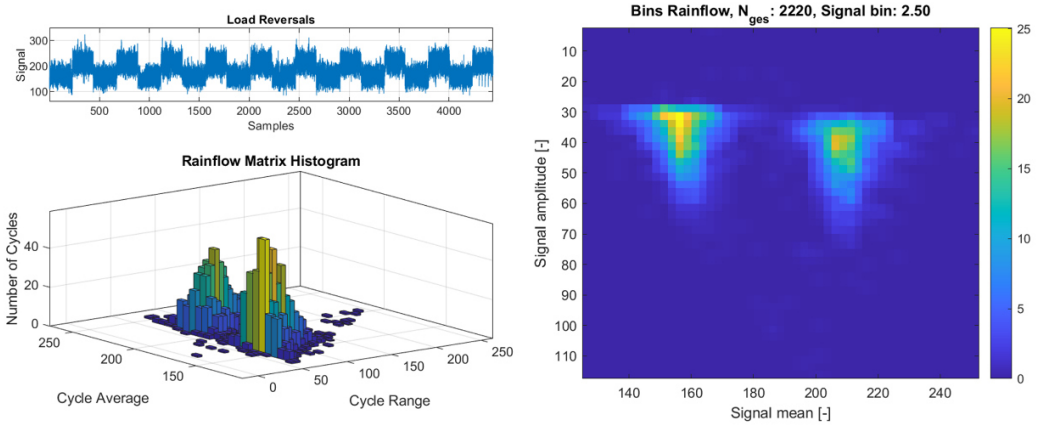

Fig. 4: Service load force timeseries and rainflow counting result as mean-amplitude pairs

The timeseries consists of twenty tumescent load blocks with almost equal block mean values. Moreover, in each load block a certain amount of overload peaks occur, especially in the second, fourth, sixth and twelfth block. The depicted timeseries signal can be used as set value in case of servo-hydraulic testing. Even though a bin width of $2.5kN$ is used in the rainflow visualization, the maximum number of load cycles per cell is about twenty-five. This is not sufficient for actual force settlement in case of the resonance test rig. Thus, a synthetic service load case has to be defined which possess sub-steps with enlarged cycle numbers.

SERVICE STRENGTH ASSESSMENT METHOD

To obtain an equivalent T-SED design value $\Delta\bar{W}_{eq}^{(t)}$ in case of variable amplitude loading, the equivalent T-SED is calculated similarly to random loading of welded components, see Eq. 1. The inverse slope values of the T-SED design curve differ from stress-based fatigue assessments, in the finite life region a slope value of $k_1 = 2.5$ and in case of high-cycle-fatigue a value of $k_2 = 12.5$ is applicable for cast steel alloy G12MnMo7-4+QT. In the equation, subscript i refers to the energy values above the knee point, subscript j references the total strain energy values below. The knee point is denoted by index k.

$$\Delta\bar{W}_{eq}^{(t)} = \left(\frac{1}{D} \cdot \frac{\sum\Delta\bar{W}_i^{(t)^{k_1}} N_i + \sum\Delta\bar{W}_k^{(t)^{(k_1-k_2)}} \cdot \sum\Delta\bar{W}_j^{(t)^{k_2}} N_j}{\sum N_i + \sum N_j} \right)^{1/k_1} \qquad \text{Eq. 1}$$

To calculate the operational strength of macroscopic imperfections based on the T-SED value, each load level has to be simulated, implying numerous simulations per specimen. Fig. 5 displays the directly simulated total strain energy density values for large-scale specimen GP80, X-plane projection, for the five different test levels of block loading as given in Table 1.

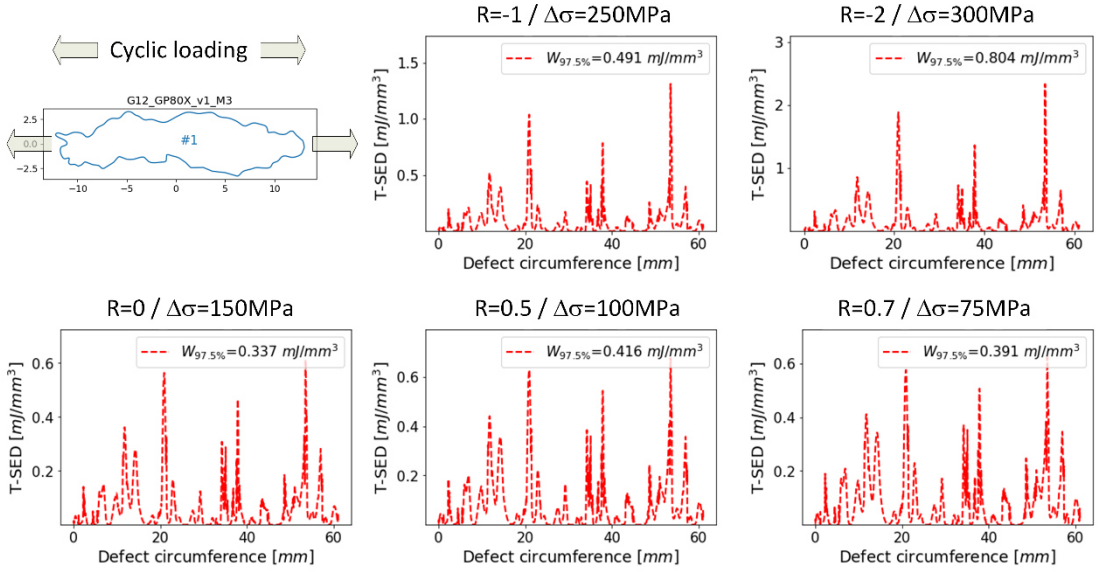

Fig. 5: Simulated T-SED distribution of each load level over projected defect circumference of large-scale specimen GP80X

A matrix of stress ratio and stress range pairs is precalculated and the needed blunt notch elasto-plastic T-SED values for service strength assessment are interpolated for each load case scenario. The T-SED simulation space in Fig. 6 is based on eighty-five data points, covering mean stress values up to $300MPa$ and stress amplitudes up to $150MPa$.

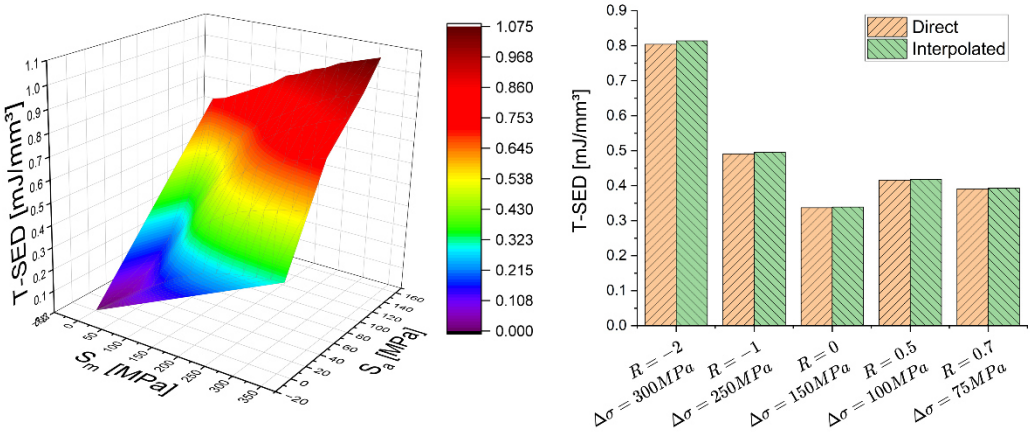

Fig. 6: Simulated T-SED distribution for large-scale specimen GP80X and mapping of directly computed strain energy density values to interpolated results

For large-scale specimen GP80, X-ray projected on X-plane, the accumulated T-SED for one period, $N = 66000$ as listed in Table 1, results in $\Delta W_{eq}^{(t)} = 0.718 mJ/mm^3$ following Eq. 1. Thus, the T-SED service life values can be calculated in a unified manner for all load steps.

MEASUREMENTS, OPERATIONAL STRENGTH RESULTS

The effect of controller settings for the resonance test rig is demonstrated for the block load case, focusing on the effect of the feedforward value at each block transition. Fig. 7 display the timeseries for three different control settings. It is recognizable that an enabled feedforward value induces transient overload peaks at specific block transitions. In detail, a pronounced resonance peak is obtained if the block transitions to lower mean stresses and higher stress ranges. It should be noted that this observation is only valid for the investigated sample geometry, material, load case block settings, and applied resonance test rig, as the overall stiffness determines this transient test behavior.

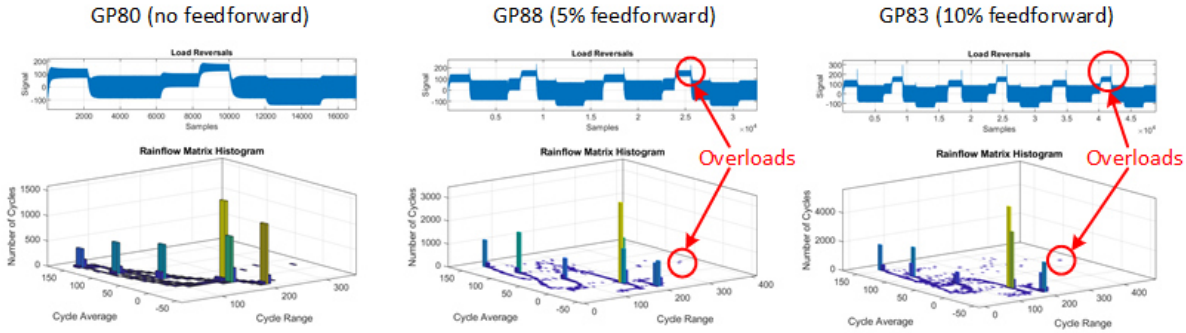

Fig. 7: Measured force timeseries and rainflow counting results of block load case for different feedforward controller settings of the resonance test rig and large-scale specimen testing

Gaussian spectrum

The variable load spectrum based on the Gaussian distribution is listed in Table 2. Fig. 8 displays the measured timeseries and rainflow counting results for this load sequence. The stress ranges are alternating, and the Gaussian load block is mirrored bathtub alike.

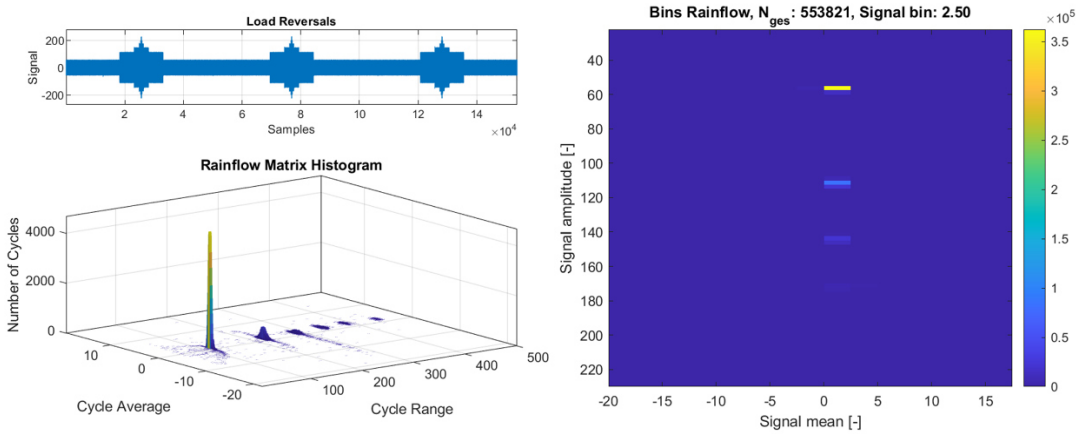

Fig. 8: Measured force timeseries and rainflow counting results of Gaussian load case (GP75)

Service load spectrum

The targeted service load spectrum in Fig. 4 possess several transient load peaks. As this spectrum is normally only suited as timeseries-based set value in servo-hydraulic testing, a modified short block cycle program was invented to approximate the depicted rainflow counting result of Fig. 4. Three different short cycle programs were developed, whereat each block consists of eight sub-steps. Thus, the total number of sub-steps counts to one-hundred and sixty for the whole period. As resonant testing needs a few seconds to reach the new load level of each sub-step, the aggregated load cycle sum of one period is increased to 75000 cycles.

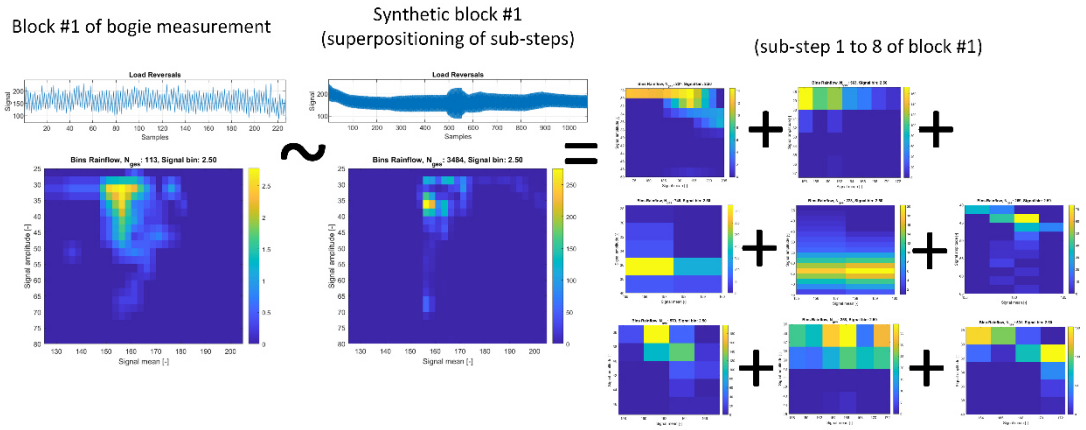

Fig. 9: Example of superposition of sub-steps to approximate bogie force timeseries

The definition of each sub-step was done by superposition of dedicated sub-step transitions and visual comparison of the rainflow results of these aggregated sub-steps to the target block. Fig. 9 illustrates the applied methodology for the first block of the bogie force measurement timeseries. Although not matching exactly, the basic distribution is similar, the main cycles are located at mean force values of about $155kN$ and the amplitudes range from 30 to $40kN$. The difference in the rainflow counting results of block-based bogie measurements and synthetic sub-step definition is caused by the entry values of the first synthetic sub-step, which steps down from a quite high mean value of $200kN$ in the last sub-step of block #20, defining the end of the bogie load period. This short cycle based sub-step definition leads to a synthetic block program in Fig. 10, which approximates the bogie measurement data of Fig. 4 satisfyingly.

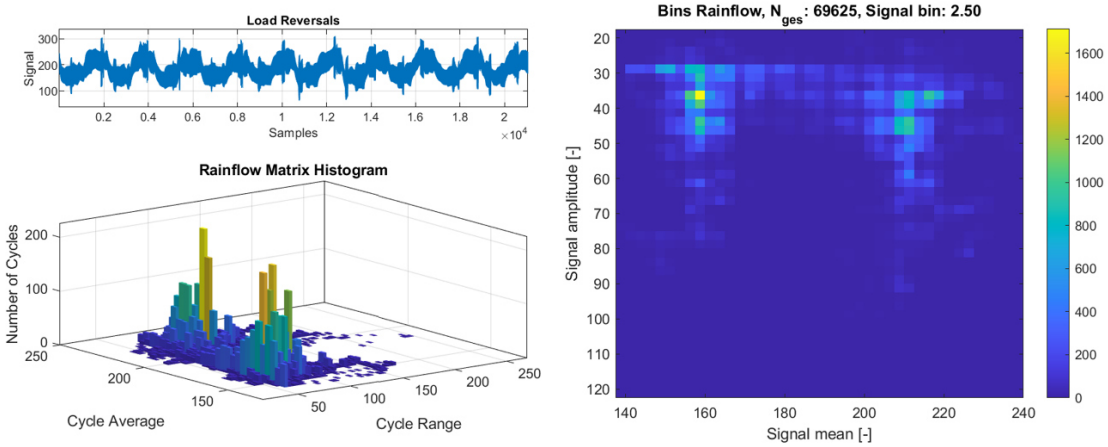

Fig. 10: Synthetic service load spectrum of bogie measurement of large-scale sample GP90

Operational strength assessment by T-SED

Forty large-scale specimens with bulk imperfections have been tested under variable amplitude loading. The operational strength test results are grouped according to their applied loading scheme, namely block loading with variable stress ratio, alternate Gaussian loading, and bogie load spectrum. Fig. 11 presents the variable amplitude results of block loading.

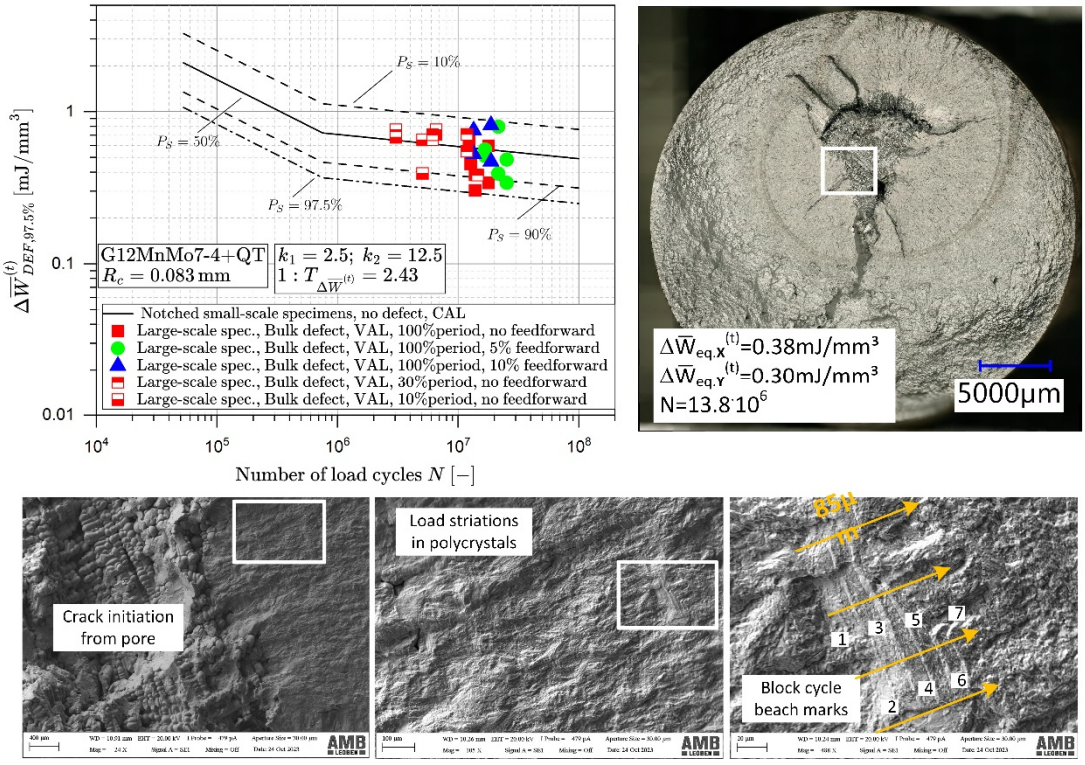

Fig. 11: Service life of block loaded large-scale samples with bulk defects (fracture surface of GP82 illustrates the crack initiation and propagation during 209 load periods)

This referenced specimen GP82 endured $N = 13.8 \cdot 10^6$ at T-SED's of $\Delta\overline{W}^{(t)}_{eq.X} = 0.38mJ/mm^3$ and $\Delta\overline{W}^{(t)}_{eq.Y} = 0.30mJ/mm^3$. The given energy values for both X-ray projections are based on the measured force history during testing, if the set values are used for T-SED calculation the

energy level would be up to twenty percent higher. This demonstrates the effect of settlement time on calculated service strength for resonant testing.

Next, Fig. 12 displays the service strength results of Gaussian block loading. As the load cycles are fully reversal, the evaluated total energy density distribution comparably increases.

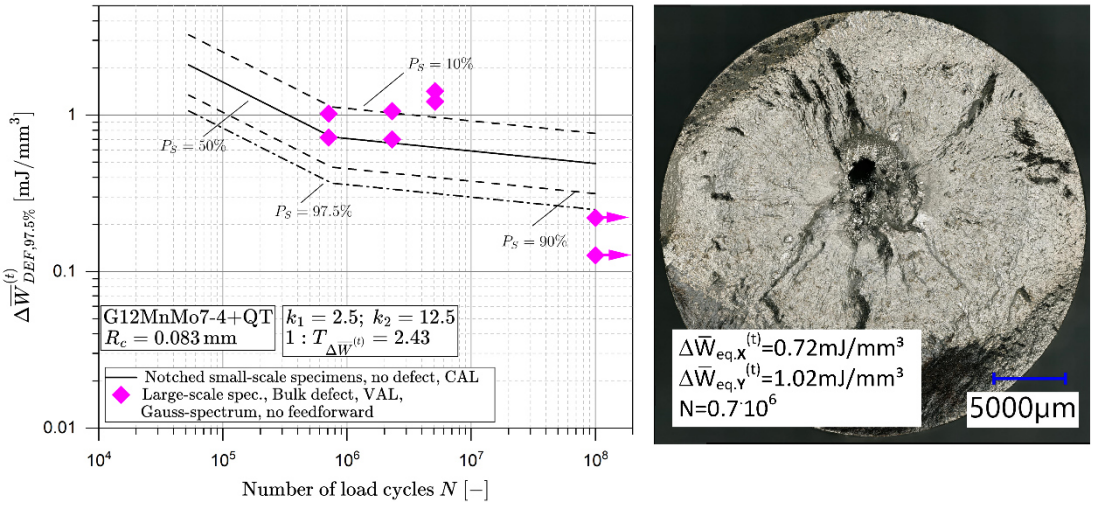

Fig. 12: Service life of Gaussian loaded large-scale samples with bulk defects (fracture surface of GP56)

This specimen was tested up to 10^8 cycles at fifty percent of the load level given in Table 2, and subsequently re-inserted at the nominal load. As crack growth was observed even for the reduced load level, it confirms that samples with pores exhibit no endurance limit.

Finally, Fig. 13 summarizes the service life results of the bogie load spectrum. Service spectrum #1 of resonant testing reaches 75% of the nominal maximum load, whereat load spectrum number #2 and number #3 differ in sub-step definition, maintaining the maximum load of Fig. 4.

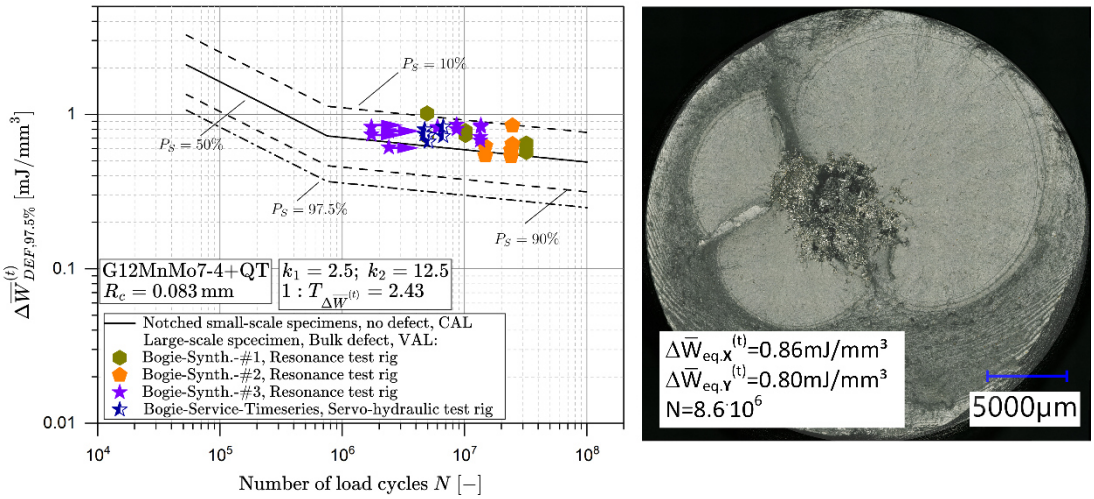

Fig. 13: Service life of bogie load cases (fracture surface of GP93 tested with synthetic load sequence #3 at resonant test rig)

To verify the resonance test rig results by approximating the bogie load spectrum with short sub-steps, compare to Fig. 10 for the synthetic load spectra, additional servo-hydraulic tests

were performed using the transient timeseries of the original Bogie force measurement data. Fig. 13 depicts that the resonance test rig and servo-hydraulic test results of large-scale specimens with bulk defects are within the same scatter band.

Summing up, the paper proofs that the service life assessment based on the elasto-plastic, total strain energy density (T-SED) is well suited to calculate the service strength for large-scale specimens with bulk defects. A damage sum of $D = 0.3$ is recommended for cast steel alloy G12MnMoV7-4+QT to meet the design curve limits under variable loading.

REFERENCES

[1] Atzori, B.:
Cracks and notches: Analogies and differences of the relevant stress distributions and practical consequences in fatigue limit predictions
Cumulative Fatigue Damage Conference, 23 (2003) No.4, pp.355-362

[2] Taylor, D.:
The theory of critical distances
Engineering Fracture Mechanics, 75 (2008) No.7, pp.1696-1705

[3] Horvath, M.; Stoschka, M.; Fladischer, S.:
Fatigue strength study based on geometric shape of bulk defects in cast steel
International Journal of Fatigue, 163 (2022) 107082, pp.9

[4] Schuscha, M.; Horvath, M.; Leitner, M.; Stoschka, M.:
Notch Stress Intensity Factor (NSIF)-Based Fatigue Design to Assess Cast Steel Porosity and Related Artificially Generated Imperfections
Metals, 9 (2019) 1097, pp.28

[5] Lazzarin, P.; Zambardi, R.:
A finite-volume-energy based approach to predict the static and fatigue behavior of components with sharp V-shaped notches
International Journal of Fracture, 112 (2001) pp.275–298

[6] Horvath, M.; Oberreiter, M.; Stoschka, M.:
Energy-Based Fatigue Assessment of Defect-Afflicted Cast Steel Components by Means of a Linear-Elastic Approach
Applied Sciences, 13 (2023) 3768, pp.23

[7] Stoschka, M.; Horvath, M.; Fladischer, S.; and Oberreiter, M.:
Study of Local Fatigue Methods (TCD, N-SIF, and ESED) on Notches and Defects Related to Numerical Efficiency
Applied Sciences, 13 (2023) 2247, pp.41

[8] Horvath, M.; Oberreiter, M.; Stoschka, M.:
A Numerically Efficient Method to Assess the Elastic–Plastic Strain Energy Density of Notched and Imperfective Cast Steel Components
Applied Mechanics, 4 (2023) No.2, pp.528–566

[9] Müllneritsch, L.:
Erarbeiten einer standardisierten Beanspruchungs-Zeit-Funktion für Kleinprobenversuche
Masterarbeit TUG; Arbeitsgruppe Betriebsfestigkeit und Schienenfahrzeugtechnik des Instituts für Maschinenelemente und Entwicklungsmethodik, Graz(2018)

Corresponding author: michael.stoschka@unileoben.ac.at